

PROTON NUCLEAR MAGNETIC RESONANCE RELAXATION MEASUREMENTS IN FROG MUSCLE

EDWARD D. FINCH *and* LOUIS D. HOMER

From the Naval Medical Research Institute, National Naval Medical Center, Bethesda, Maryland 20014

ABSTRACT Proton nuclear magnetic resonance (NMR) relaxation measurements are reported for frog muscle as a function of temperature and Larmor frequency. Each $T_{1\rho}$, T_2 , and T_1 measurement covered a time domain sufficient to identify the average relaxation time for most intracellular water. Using regression analysis the data were fit with a model where intracellular water molecules are exchanging between a large compartment in which mobility is similar to ordinary water and a small compartment in which motion is restricted. The regression results suggest that: the restricted compartment exhibits a distribution of motions skewed toward that of free water; the residence time of water molecules in the restricted compartment is approximately 1 ms; and, the activation entropy for some water molecules in the restricted compartment is negative.

INTRODUCTION

Nuclear magnetic resonance (NMR) studies can provide valuable information about the dynamic properties of tissue water. The parameters that can be measured with pulsed NMR techniques include the spin-lattice relaxation time in the laboratory frame (T_1) and in the rotating frame ($T_{1\rho}$), the spin-spin relaxation time (T_2), and the diffusion constant (D).

Early investigators (1, 2) found that T_1 and T_2 for muscle water were much shorter than in ordinary water. The reduced T_1 and T_2 values indicated that the rotational and translational mobility of muscle water was nearly two orders of magnitude lower than ordinary liquid water. However, subsequent measurements of D showed unequivocally that the average translational mobility of most muscle water is reduced only by a factor of two (3-6).

Today, it is generally believed that NMR relaxation times reflect the reduced mobility of hydrated or bound water (3, 7-9). NMR relaxation times may prove to be a very sensitive tool for studying the dynamic properties of hydrated water if adequate models are developed for their interpretation. Outhred and George (8) found that muscle water T_1 data measured as a function of temperature and Larmor frequency were consistent with a model where a few percent of muscle water had a distribution of mobilities between those of ice and liquid water; in this model, the motional freedom

of the remaining muscle water ($\sim 97\%$) was considered to be similar to ordinary water in agreement with measured diffusion constants.

The T_1 measurements of Outhred and George (8) were most sensitive to the faster motions in hydrated water due to the range of Larmor frequencies used in their study. They did measure T_2 which is sensitive to slower motions and found little dependence of this parameter upon either Larmor frequency or temperature. They did not use T_2 data in their model development.

Koenig and Shillinger (10) have shown that T_1 measurements in protein solutions can provide information about the slower motions of hydrated water if relaxation occurs in magnetic fields approaching zero; facilities for making these measurements are not commonly available. An alternative method of obtaining information about slower motions is to measure spin-lattice relaxation in the rotating frame. $T_{1\rho}$ measurements in mouse muscle at room temperature have been reported by Thompson et al. (11).

In the present study, T_1 , T_2 , and $T_{1\rho}$ have been measured in frog muscle as a function of temperature and Larmor frequency. The range of Larmor frequencies covered in the laboratory frame was not as extensive as in the T_1 measurements of Outhred and George (8). However, Larmor frequencies in the laboratory and rotating frame covered a span of over 10^4 . By combining all $T_{1\rho}$, T_1 , and T_2 data in a regression analysis, a new quantitative model of muscle water has been developed.

METHODS AND MATERIALS

In liquid water and ice, NMR relaxation occurs via dipolar interactions, mainly intramolecular, between water protons. These interactions are modulated by the motion of the water molecules; this motion is characterized by a correlation time, τ , which is a measure of the time required for a molecule to undergo an incremental motion (12-14). Expressions for the T_1 , T_2 , and $T_{1\rho}$ relaxation times are, assuming intramolecular interactions only,

$$\frac{1}{T_1} = C \left[\frac{2\tau}{1 + \omega_0^2 \tau^2} + \frac{8\tau}{1 + 4\omega_0^2 \tau^2} \right], \quad (1)$$

$$\frac{1}{T_2} = C \left[3\tau + \frac{5\tau}{1 + \omega_0^2 \tau^2} + \frac{2\tau}{1 + 4\omega_0^2 \tau^2} \right], \quad (2)$$

$$\frac{1}{T_{1\rho}} = C \left[\frac{3\tau}{1 + 4\omega_1^2 \tau^2} + \frac{5\tau}{1 + \omega_0^2 \tau^2} + \frac{2\tau}{1 + 4\omega_0^2 \tau^2} \right], \quad (3)$$

where: ω_0 is the NMR Larmor angular frequency in the constant magnetic field, H_0 ; ω_1 is the Larmor frequency in the rotating frame in the presence of a radio frequency (RF) field, H_1 ; and C is a constant.

Both ω_0 and ω_1 are variable parameters. From Eqs. 1-3, we see that if τ is such that $\omega_0 \tau > 1$, information about motion can be obtained by studying the ω_0 dependence of T_1 . The parameter ω_0 can commonly be varied over a range of about 10^7 - 10^9 rad/s. In pure water, τ is so small ($< 10^{-11}$ s) that $\omega_0 \tau \ll 1$ even at the highest attainable ω_0 values; this explains (See Eqs. 1-3) why $T_1 = T_2$ in pure water. These equations also show that for all τ values, $T_2 \leq T_{1\rho} \leq T_1$.

Additional information about mobility can be obtained by measuring the NMR relaxation time as a function of temperature. A change in temperature produces a change in rotational freedom and a corresponding change in τ . For example, T_1 increases with increasing temperature (decreasing τ) if τ is in the range such that $\omega_0\tau < 1$ and decreases with increasing temperature if τ is such that $\omega_0\tau > 1$. An analogous temperature dependence is expected for $T_{1\rho}$ for τ values giving $\omega_1\tau < 1$ and $\omega_1\tau > 1$, respectively. $T_{1\rho}$ measurements made with $\omega_1 \sim 10^5$ to 10^7 rad/s can provide information about the longer correlation times that we believe to be characteristic of some intracellular water. In the present study, ω_0 has been varied over a range from 125.7×10^6 rad/s to 172.8×10^6 rad/s and ω_1 over a range of 3.5×10^4 rad/s to 57.9×10^4 rad/s.

The Spectrometer

A phase coherent spectrometer constructed in our laboratory was employed for all measurements in this study. The sample probe contained a single coil for transmitting and receiving. The recovery time of the RF receiver after a large RF pulse was approximately 40 μ s. The probe was completely shielded to eliminate RF interference in the magnet regulator, a Magnion model FFC-4 (Magnion, Burlington, Mass.), during the long RF pulses required for rotating frame measurements. The separation, width, and amplitude of the RF pulses were monitored continuously at the coil with a high voltage Tektronix probe (P601SX1000) and a Tektronix oscilloscope (model 454A) (Tektronix, Inc., Beaverton, Ore.).

To avoid problems of nonlinear video detection of the NMR signal, all data were obtained directly with a model 454A Tektronix oscilloscope; i.e., the amplified RF echo and induction decay signals were observed directly without video detection. To insure that the spectrometer was operating properly, relaxation time measurements were routinely made on a standard glycerin sample.

Spin-Spin Relaxation Measurements

Most investigators have reported a single T_2 (~ 45 ms) for muscle water. However, recent studies over an extended time domain have identified, in addition, a shorter relaxation time (< 5 ms) and a longer relaxation time (~ 200 ms) (15, 16). The intermediate and short relaxation times have been attributed to intracellular water. The longest relaxation time has been identified with extracellular water.

In the present study, T_2 was obtained with the spin-echo technique using the $\pi/2$ - π pulse sequence (17); the amplitude, $M(t)$, of the spin-echo is monitored as a function of t , the time interval between $\pi/2$ and π pulses. T_2 and $M(t)$ are related by the function,

$$M(t) = M(0) \exp(-2t/T_2). \quad (4)$$

The range of $2t$ in this study extended from approximately 2 ms to 100 ms; this was sufficient to characterize the major intermediate relaxation component in muscle with $T_2 \sim 45$ ms. A typical spin-echo decay curve is shown in Fig. 1.

Spin-Lattice Relaxation in the Rotating Frame

Measurements were made using the Solomon technique (18); the sample is subjected to a $\pi/2$ pulse which is followed immediately by a second pulse of amplitude, H_1 , and duration, t . The second pulse is phase shifted by 90° . $T_{1\rho}$ is obtained by monitoring the amplitude, $M(t)$, of the RF induction decay following the second pulse:

$$M(t) = M(0) \exp(-t/T_{1\rho}). \quad (5)$$

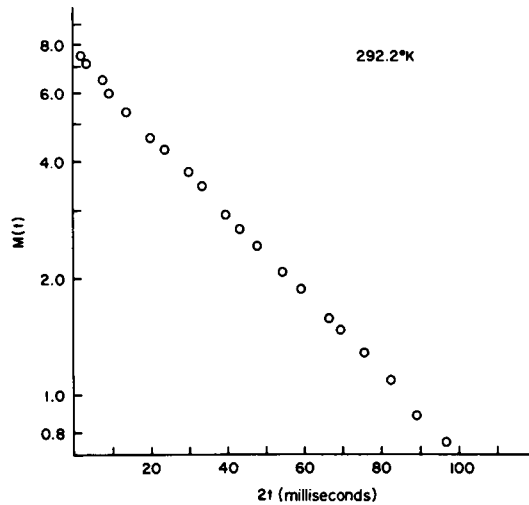


FIGURE 1 Spin echo amplitude $M(t)$, plotted against $2t$ where t is the time between a π and $\pi/2$ pulse. The slope of this semilog plot is proportional to T_2 .

The range of t values in this study was ~ 0.1 ms to 150 ms. A typical decay curve is shown in Fig. 2. There was usually evidence of a short $T_{1\rho}$ (< 5 ms) representing perhaps 5% of the water which, presumably, corresponds to the small intracellular fraction previously reported from T_2 observations (16). The remaining data could be characterized by a single $T_{1\rho}$ which we attribute to the large intracellular water fraction determining the T_2 data in Fig. 1. Since $T_{1\rho} > T_2$ the fraction with $T_2 \sim 200$ ms attributed to extracellular water (16), could not be observed within our limited measurement time domain.

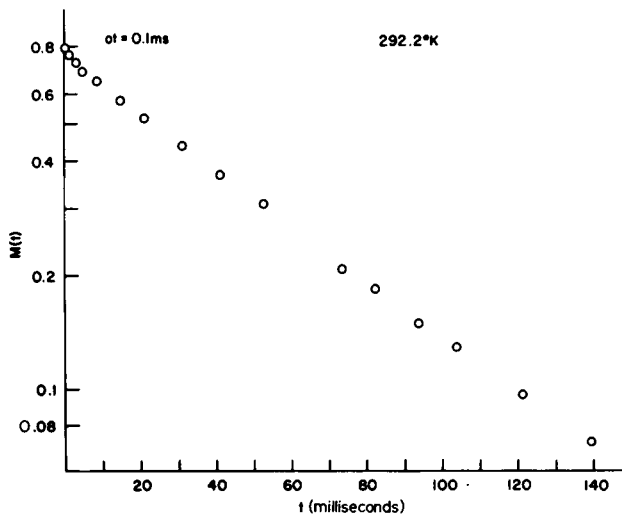


FIGURE 2 Induction signal amplitude, $M(t)$, plotted against t , the length of the preceding pulse. The slope of this semilog plot is proportional to $T_{1\rho}$.

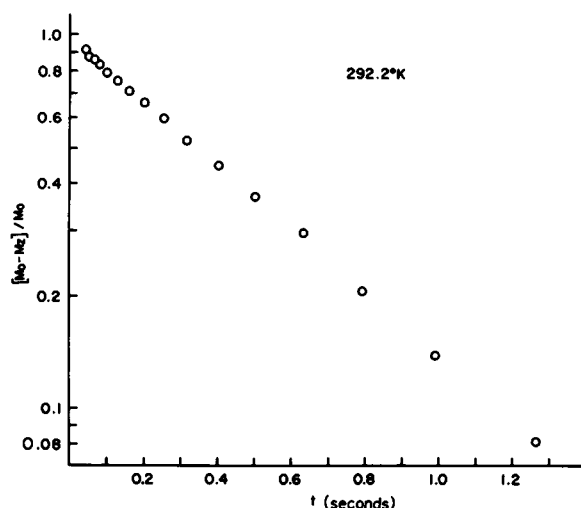


FIGURE 3 Normalized induction signal amplitude, $[M_0 - M_z]/M_0$ plotted against t , the time between $\pi/2$ pulses. The slope of this semilog plot is proportional to T_1 .

Spin-Lattice Relaxation

T_1 measurements were made by monitoring the amplitude of the induction signal, M_z , following a $\pi/2$ pulse. M_z is related to T_1 by the relationship (19),

$$M_z = M_0(1 - \exp(-t/T_1)), \quad (6)$$

where t is the time between $\pi/2$ pulses.

The range of t values in this study was ~ 25 ms to ~ 1.2 s; the lower limit was set by interference from $\pi/2$ - $\pi/2$ spin-echoes and the upper limit by signal to noise. A typical decay curve is shown in Fig. 3. The data can be characterized by a single exponential which we attribute to the large intracellular fraction of muscle water; i.e., the same fraction identified with the T_2 decay in Fig. 1 and the $T_{1\rho}$ decay in Fig. 2.

Sample Preparation and Handling

Rana pipiens frogs were obtained from Southwestern Scientific, Tucson, Ariz. They were kept in an aquarium (55°F) without food. After killing the frog by pithing, the gastrocnemius muscle was excised, blotted to remove excess water, inserted into a test tube (12 mm OD), and placed in the NMR sample probe for measurements. NMR measurements were made on frogs kept less than 1 wk after delivery.

Sample temperature was regulated with a Varian Temperature Controller (Varian Associates, Palo Alto, Calif.). Temperatures were monitored with a calibrated YSI needle thermistor immediately before and after each NMR measurement. The uncertainty in sample temperature was less than $\pm 1/2^\circ\text{C}$ across the sample.

For a given sample at a particular temperature, all NMR measurements (T_2 , T_1 , and $T_{1\rho}$ as a function of ω_1) were completed within 2 h after the animal was killed. Each muscle was checked for excitability after the NMR measurements were completed. As an additional check on viability a T_2 measurement was routinely made at the beginning of the NMR measurements and then repeated after T_1 and $T_{1\rho}$ measurements were completed.

RESULTS

The majority of the measurements were obtained with a Larmor frequency of 23.3 MHz; these data are plotted in Fig. 4 to show the temperature dependences of $T_{1\rho}$, T_2 , and T_1 . Results for other Larmor frequencies are listed in Table I; the uncertainty in the relaxation times is estimated to be $\pm 5\%$. The effect of the slowly relaxing fraction, attributed to extracellular water (16), on this determination of the intracellular relaxation times is not known. However, judging from straightness of the decay curves such corrections would be smaller than the stated uncertainty.

We see that T_1 increases with increasing temperature, indicating, from Eq. 1, motional narrowing and $\omega_0\tau < 1$ or $\tau < 10^{-9}$ s. An examination of the T_1 data in Table I and Fig. 4 also shows, in agreement with the previous studies of Outhred and George (8), that T_1 is a function of the Larmor frequency; Eq. 1 indicates that this can only be the case if $\omega_0\tau > 0.1$; i.e., τ must be greater than $\sim 10^{-10}$ s. Therefore, T_1 seems to be dominated by motions with correlation times in the range 10^{-9} to 10^{-10} s.

Fig. 4 shows that $T_{1\rho}$ is much smaller than T_1 , is a function of ω_1 , and increases with temperature. From Eq. 3 and arguments similar to those in the previous paragraph, $T_{1\rho}$ appears to be determined mainly by motional correlation times ranging

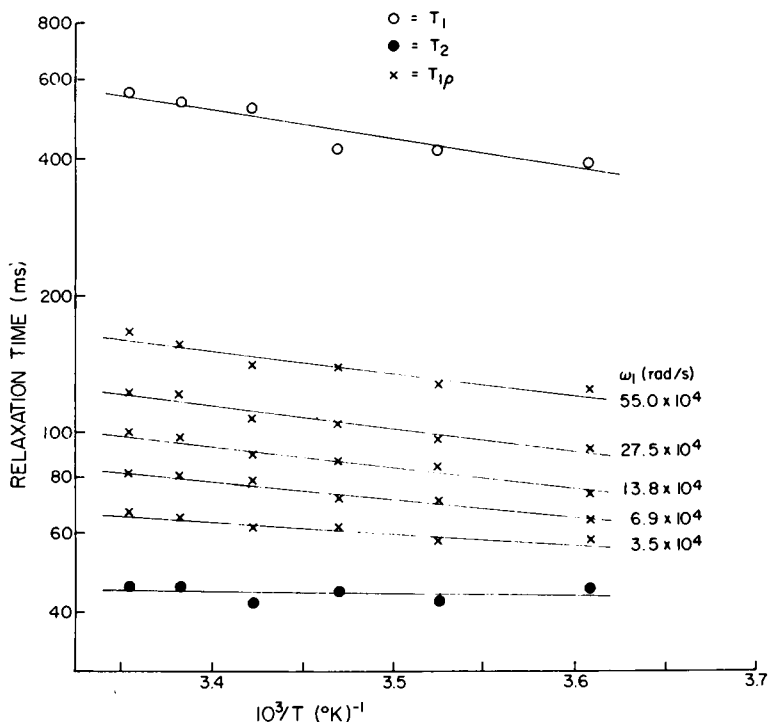


FIGURE 4 Temperature dependence of $T_{1\rho}$, T_1 , and T_2 proton NMR relaxation times of muscle water. All data shown were obtained at $\omega_0 = 146.4 \times 10^6$ rad/s. The uncertainty in data is estimated to be $\pm 5\%$.

TABLE 1*
 T_1 , T_2 , AND $T_{1\rho}$ PROTON NMR RELAXATION MEASUREMENTS
 ON FROG GASTROCNEMIUS MUSCLE

Temperature	$\omega_1 \times 10^{-4}$	$\omega_0 \times 10^{-6}$	$i \dagger$	$T_i \S$
$^{\circ}K$	<i>rad/s</i>	<i>rad/s</i>		<i>ms</i>
295.7	0	172.8	2	44
295.7	0	172.8	1	700
295.7	55.0	172.8	3	180
295.7	27.5	172.8	3	137
295.7	13.8	172.8	3	99
295.7	6.9	172.8	3	83
295.7	3.5	172.8	3	72
287.5	0	166.5	2	46
287.5	0	166.5	1	490
287.5	49.4	166.5	3	131
287.5	37.1	166.5	3	114
287.5	24.7	166.5	3	107
287.5	11.3	166.5	3	81
287.5	0	125.7	2	47
287.5	0	125.7	1	390
287.5	57.9	125.7	3	135
287.5	43.4	125.7	3	127
287.5	28.9	125.7	3	112
287.5	14.5	125.7	3	92

*Data obtained with ω_0 values other than 146.4×10^6 rad/s.

\dagger The index i has values of 1, 2, and 3 for T_1 , T_2 , and $T_{1\rho}$, respectively.

\S The $\pm 5\%$ uncertainty in these data results from the uncertainty in the slope of the corresponding relaxation decay curves.

from 10^{-5} s for the smallest ω_1 to 10^{-7} s for the largest ω_1 . Together the $T_{1\rho}$ and T_1 data indicate a range of correlation times in intracellular water extending from 10^{-5} s to 10^{-10} s).

For T_1 , those correlation times shorter than $1/\omega_0$ would cause T_1 to increase with increasing temperature while those longer than $1/\omega_0$ would cause T_1 to decrease with increasing temperature. Similarly, with increasing temperature, correlation times shorter than $1/\omega_1$ and longer than $1/\omega_1$ would cause $T_{1\rho}$ to increase and decrease, respectively. Since no minima are evident and both T_1 and $T_{1\rho}$ increase with increasing temperature, the distribution of correlation times appears to be skewed toward shorter correlation times.

Thompson et al. (11) measured the ω_1 dependence of $T_{1\rho}$ in mouse muscle at room temperature in the range $\omega_1 \sim 10^5$ to 10^7 rad/s. Their results showed approximately the same ω_1 dependence as our data at room temperature. They analyzed their data using an expression of the form,

$$1/T_{1\rho} = R + (A\tau_c/[1 + 4\omega_1^2\tau_c^2]). \quad (7)$$

The second term in this expression resembles the first term in Eq. 3. However, these

authors identified τ_e with the exchange correlation time of water protons rather than the rotational correlation time of water molecules. The constant A is defined only as a measure of the "interaction which is being modulated by the exchange"; the nature of this interaction is not identified. The constant R is identified with the "proton relaxation rate in the absence of exchange" which must be the dipolar relaxation rate given by Eq. 3. These authors treat R as a constant neglecting its ω_1 dependence which is appreciable in their experiment for rotational correlation times in the range of 10^{-5} s to 10^{-7} s. Interestingly, a $\tau_e = 5 \times 10^{-6}$ s was obtained in their analysis.

The proton exchange correlation time in liquid water is approximately 10^{-3} s (20). For water of hydration it appears that the proton exchange correlation time may be decreased by as much as an order of magnitude (Woessner, D. E., unpublished results). However, an exchange correlation time of 5×10^{-6} s for muscle water clearly seems out of the range of expectations. We believe that the τ_e in Eq. 7 can be more reasonably identified with the rotational correlation time of water molecules.

ANALYSIS

We have chosen a two-compartment model for analysis; it assumes that the data may be represented by a large compartment of free water with a correlation time, τ_w , and a small compartment with restricted motions and a distribution of correlation times. The model also assumes that water molecules are exchanging between these two compartments in a time short compared with the NMR observation time. With these assumptions, the calculated relaxation rate (the reciprocal of the relaxation time) is given by a weighted average of the rates in each compartment (16):

$$(1/T_i)_{\text{cal}} = (F_w/T_{iw}) + [(1 - F_w)/(T_{iR} + R_i)]. \quad (8)$$

The index i has values of 1, 2, and 3 for T_1 , T_2 , and $T_{1\rho}$, respectively. T_{iw} and T_{iR} represent the calculated relaxation times in the free and restricted compartments, respectively. R_i is the residence time of a water molecule in the restricted compartment. F_w and $(1 - F_w)$ represent the fractions of water in free and restricted compartments, respectively.

Since T_{iw} is characterized by a single correlation time (τ_w) it can be calculated directly from Eqs. 1, 2, or 3. The relaxation rate in the restricted compartment is calculated assuming a distribution of M discrete correlation times:

$$\frac{1}{T_{iR}} = \sum_{j=1}^M \frac{f(j)}{T_i(\tau_j)}. \quad (9)$$

Again the index i takes on values of 1, 2, and 3 and the $T_i(\tau_j)$'s are calculated from Eqs. 1-3. The distribution weighting function, $f(j)$, is taken as,

$$f(j) = \exp(jB_1 + j^2B_2) / \sum_{j=1}^M \exp(jB_1 + j^2B_2). \quad (10)$$

The choice of this discrete distribution greatly simplifies computations and should provide an approximate picture of any continuous distribution.

The temperature dependence of motion in both compartments is assumed to depend upon the free energy of activation, ΔG^* , in the same manner as the dielectric relaxation time in liquid water (21):

$$\tau = (h/3.7kT) \exp(\Delta G^*/RT). \quad (11)$$

In this expression, h is Planck's constant, k is Boltzmann's constant, R is the ideal gas constant, and T is the absolute temperature. The factor of 3.7 comes from the experimental observation that the NMR correlation time in free water (τ_w) is smaller than the dielectric relaxation time in free water by a factor of 3.7 (21). ΔG_w^* is calculated from the activation enthalpy (ΔH_w^*) and entropy (ΔS_w^*) obtained from dielectric relaxation measurements in free water (21) ($\Delta H_w^* = 4.2$ kcal/mol, $\Delta S_w^* = 6.1$ cal/mol-deg).

We assume that each discrete correlation time, τ_j , in the restricted compartment is characterized by an activation free energy, ΔG_j^* . The free energies are calculated from an expansion in temperature about the midrange of our observations (288.2°K):

$$\Delta G_j^* = (j - B_3)B_4 + (T - 288.2)(B_5 + (j - B_3)B_6). \quad (12)$$

Note that the activation enthalpy, ΔH_j^* , and activation entropy, ΔS_j^* , can be defined as follows,

$$\begin{aligned} \Delta H_j^* &= \Delta G_j^* \quad (\text{evaluated at } T = 0) \\ -\Delta S_j^* &= (\Delta G_j^* - \Delta H_j^*)/T \quad (T \neq 0). \end{aligned} \quad (13)$$

A similar expansion is used to estimate the temperature dependence of the residence time of a water molecule in the restricted compartment:

$$R_i = B_7 + B_8(T - 288.2). \quad (14)$$

The parameters B_1 through B_8 can be calculated by a least squares fit to the data. The computer program we have used adjusts nine parameters (B_1 through B_8 plus F_w) to minimize the sum of square errors (SSE) from N observations.

$$\text{SSE} = \sum_{i=1}^{N=61} [\log(1/T_i)_{\text{obs}} - \log(1/T_i)_{\text{cal}}]^2. \quad (15)$$

The 61 observations represent the relaxation data points in Fig. 4 and Table I. The iterative algorithm we have used is a blend of the gradient method (22), the method of Hartley (23), and the Marquardt algorithm (24).

Estimating the Constant C

Before beginning the regression procedure, the constant C in Eqs. 1-3 had to be approximated. For intramolecular interactions this parameter can be defined exactly (13).

$$C = (3/4)\gamma^4\hbar^2/20r^6, \quad (16)$$

where γ is the nuclear gyromagnetic ratio, \hbar is Planck's constant divided by 2π , and r is the distance between protons on a water molecule. Using a value of $r = 1.58 \text{ \AA}$, the intramolecular C is calculated to be $0.549 \times 10^{10} \text{ s}^{-2}$.

Unlike intramolecular interactions, intermolecular interactions are dominated by the translation of water molecules (13). Eisenberg and Kauzmann (25) have shown that rotation and translation of water molecules in water are strongly coupled; following Resing (26) and Outhred and George (8), we will make the approximation that a single correlation time can be used to characterize both motions. In this case, $3C$ is equal to the rigid lattice second moment, σ . From the measured value of σ , $2.4 \times 10^{10} \text{ s}^{-2}$ (14, 27), C becomes $\sim 0.8 \times 10^{10} \text{ s}^{-2}$.

Regression Results

Initial regressions were carried out with C fixed at the intramolecular value, $0.549 \times 10^{10} \text{ s}^{-2}$. Regressions were run using different numbers of components in the distribution of correlation times for the restricted compartment. The best fit occurred with five components ($M = 5$); this fit was significantly better than either four or six components. The standard deviation for this regression ($M = 5$) fit was 0.051; this

TABLE II
REGRESSION RESULTS FOR $M = 5$

Parameter	Estimate	SE
F_w	0.972	0.001
B_1	-2.16	0.16
B_2	0.144	0.035
B_3	-3.37	0.13
B_4	13.32×10^2	29.0
B_5	-86.0	16.0
B_6	16.6	3.1
B_7	0.80×10^{-3}	0.14×10^{-3}
B_8	0.70×10^{-5}	0.71×10^{-5}

This table shows the regression results when the restricted compartment contained five discrete correlation times. B_4 is in calories per mole. B_5 and B_6 are in calories per mole-degree. B_7 is in seconds and B_8 in seconds per degree centigrade. All other parameters are dimensionless. SE represents the standard error of each parameter. The standard deviation for this regression fit was 0.051.

corresponds to our expectations based on the uncertainty in the experimental observations. The regression results for the five component distribution are listed in Table II.

Other regressions were run with C increased to $0.8 \times 10^{10} \text{ s}^{-2}$. The results were similar to those for the smaller C with only minor changes in the estimates of parameters.

DISCUSSION

From Table II, we find that our model predicts that the free compartment contains 97% of the water and the restricted compartment contains 3%. The parameter B_7 indicates that water molecules (at 288.2°K) spend approximately 0.8 ms in the restricted compartment before returning to the free compartment. At 288.2°K, the calculated values of T_1 , T_2 , and $T_{1\rho}(\omega_1 = 55 \times 10^4 \text{ s}^{-2})$ in the restricted compartment are 13 ms, 0.4 ms, and 0.9 ms, respectively. The T_1 , T_2 , and $T_{1\rho}$ relaxation times in the free compartment are of the order of several seconds. We see that relaxation in the restricted compartment can have a dramatic effect on the observed relaxation time even though this compartment is small compared with the free compartment.

The averaging of relaxation in the two compartments can only occur if observation times are long compared to the residence time in the restricted compartment; i.e., long compared with R_1 . We would predict that measurements made at times less than or equal to R_1 would allow the direct observation of relaxation in the restricted com-

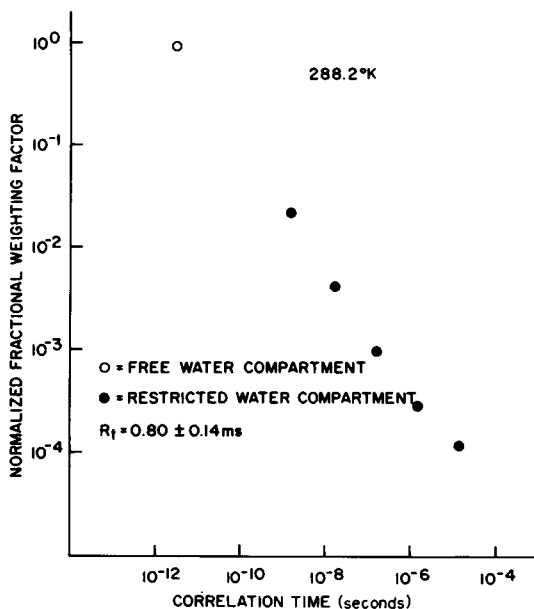


FIGURE 5 Fractional weighting factors are plotted against the corresponding correlation time for the five-component distribution for the restricted compartment.

partment. Although not well defined, the short intracellular T_2 recently observed in muscle was approximated to be 0.42 ms (16). We believe that this T_2 can be identified, at least in part, with the restricted compartment in our model.

Distribution of Correlation Times

Fig. 5 shows the normalized fractional distribution of correlation times calculated from the regression results in Table II. As expected, the distribution is strongly skewed toward the free water correlation time. It has the same general shape as the truncated continuous distribution reported by Outhred and George (8); Walter and Hope (28) were the first to predict a skewed distribution.

Residence Time

The residence time R_i at 288.2°K is equal to parameter $B_7 = 0.80 \pm 0.14$ ms. The temperature dependence of R_i (given by parameter B_8) is not well defined; however, over the temperature spread of our data the uncertainty in B_7 and B_8 indicates that R_i varies between 0.5 ms and 1.5 ms. Since R_i is the same order of magnitude as T_2 and $T_{1\rho}$ in the restricted compartment, we see from Eq. 7 that it contributes significantly to the observed average T_2 and $T_{1\rho}$ relaxation times. The R_i contribution is greatest for T_2 , decreases for $T_{1\rho}$ as ω_1 is increased, and is negligible for T_1 .

The decision to assign a single residence time for the restricted compartment was made to facilitate computations. Since a distribution of residence times seems more plausible physically, we might consider the calculated value as an average. The uncertainty in the temperature dependence of R_i may indicate the need for a distribution of residence times.

Activation Parameters

The thermodynamic activation parameters, ΔH^* and ΔS^* for the distribution have been calculated from the regression results in Table II and plotted in Fig. 6. When calculating the free energy of activation we find that ΔG_j^* varies linearly from the free water value of 2.4 kcal/mol to approximately 11.5 kcal/mol for the distribution component with the longest correlation time $\sim 10^{-5}$ s. The activation energy for rotational and translational motions in ice is ~ 13 kcal/mol with a correlation time $\sim 10^{-5}$ s (29). It might seem reasonable, therefore, to think of the longer correlation times in our distribution as being ice-like. However, the difference between the ΔG^* of free ice and free water is due mainly to an increase in ΔH^* (29) while in our distribution it is due entirely to a decrease in ΔS^* .

No independent data are available on the entropy of activation of motionally restricted intracellular muscle water. However, some information is available on other systems. For example, Harvey and Hoekstra (30) have reported dielectric relaxation measurements for water adsorbed on lysozyme. Their data indicate an average entropy of activation of -27.3 cal/mol-deg for the first hydration layer. These authors attribute the depressed freezing point of this water ($\sim -80^\circ\text{C}$) to this decrease in ΔS^* ; a small fraction of muscle water also exhibits a greatly depressed freezing point

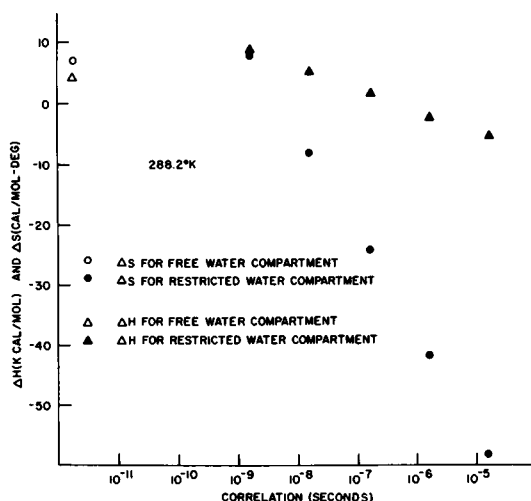


FIGURE 6 Activation enthalpy and entropy for free and restricted compartments are plotted against the correlation time obtained for each component of the distribution.

($\sim -80^{\circ}\text{C}$) which can not be attributed to either eutectic depression or supercooling (15, 31).

Without intermolecular hydrogen bonding, H_2O would be expected to freeze at about -90°C (32); under these conditions water molecules are said to be *unassociated*. The greatly depressed freezing point of water absorbed on alumina and silica gel has been attributed to unassociated water molecules (33); the water adsorbed on silica appears to be more ordered than bulk water (lower entropy) and that adsorbed on alumina less ordered.

In another NMR study, Kuntz and Brassfield (34) found a negative activation entropy (-10 cal/mol-deg) for water bound to bovine serum albumin. They made no attempt to assign any physical significance to their observation.

In a recent study of dielectric relaxation of water in gelatine solutions, Masszi (35) reported evidence of increased dielectric relaxation times for water closely associated with the protein. He attributes this not to an increase in ΔH^* (stronger hydrogen bonding) but, rather, to a decrease in the ΔS^* activation entropy.

SUMMARY

T_1 , T_2 , and $T_{1\rho}$ relaxation times have been measured in frog muscle as a function of temperature and Larmor frequency. The range of Larmor frequencies extended from 3.5×10^4 rad/s in the rotating frame to 1.73×10^8 rad/s in the laboratory frame. Assuming that the relaxation mechanisms are due to dipolar interactions, the data analysis clearly indicates a distribution of correlation times for muscle water ranging from $\sim 10^{-5}$ to $\sim 10^{-11}$ s and skewed toward the latter value.

All relaxation data (61 values) have been simultaneously fit with a model which as-

sumes that water molecules are exchanging between two compartments, one with unrestricted motions similar to ordinary water, and one with a distribution of restricted motions. Predictions of the model are consistent with available experimental evidence concerning the dynamic properties of muscle water. In particular, the R_1 and T_2 parameters calculated for the restricted compartment are in agreement with recent measurements over an extended time domain (16).

The opinions in this paper are those of the authors and do not necessarily reflect those of the Navy Department or the naval service. The animals used in this study were handled in accordance with the provisions of Public Law 89-544 as amended by Public Law 91-579, the "Animal Welfare Act of 1970," and the principles outlined in the "Guide for the Care and Use of Laboratory Animals," U.S. Department of Health, Education, and Welfare Publication No. (NIH) 73-23.

Received for publication 6 May 1974 and in revised form 19 July 1974.

REFERENCES

1. BRATTON, C. B., A. L. HOPKINS, and J. W. WEINBERG. 1965. *Science (Wash. D.C.)* **147**:738.
2. COPE, F. W. 1969. *Biophys. J.* **9**:303.
3. FINCH, E. D., J. F. HARMON, and B. H. MULLER. 1971. *Arch. Biochem. Biophys.* **147**:299.
4. ABETSEDARSKAYA, L. A., F. G. MIFTAKHUTDINOVA, and V. D. FEDOTOV. 1968. *Biofizika*. **13**:630.
5. HANSEN, J. R. 1970. *Biophys. Acta*. **230**:482.
6. CHANG, D. C., H. E. RORSCHACH, B. L. NICHOLS, and C. F. HAZLEWOOD, 1973. *Ann. N. Y. Acad. Sci.* **204**:434.
7. WOESSNER, D. E., and B. S. SNOWDEN. 1973. *Ann. N. Y. Acad. Sci.* **204**:113.
8. OUTHRED, R. K., and E. P. GEORGE. 1973. *Biophys. J.* **13**:97.
9. COOKE, R., and R. WIEN. 1971. *Biophys. J.* **11**:1002.
10. KOENIG, S. H., and W. E. SCHILLINGER. 1969. *J. Biol. Chem.* **244**:3283.
11. THOMPSON, R. T., R. R. KNISPEN, and M. M. PINTAR. 1973. *Chem. Phys. Lett.* **22**:335.
12. ABRAGAM, A. 1961. Principles of Nuclear Magnetism. Oxford University Press, Clarendon.
13. CARRINGTON, A., and A. D. McLACHLAN. 1967. Introduction to Magnetic Resonance. Harper & Row, Publishers, New York. 192.
14. BLOEMBERGEN, N. E., E. M. PURCELL, and E. M. POUND. 1948. *Phys. Rev.* **73**:679.
15. BELTON, P. S., R. R. JACKSON, and K. J. PACKER. 1972. *Biochim. Biophys. Acta*. **286**:16.
16. HAZLEWOOD, C. F., D. C. CHANG, B. L. NICHOLS, and D. E. WOESSNER. 1974. *Biophys. J.* **14**:583.
17. CARR, H. Y., and E. M. PURCELL. 1954. *Phys. Rev.* **94**:630.
18. SOLOMON, I. 1959. *C.R. Acad. Sci.* **248**:92.
19. FARRAR, T. C., and E. D. BECKER. 1971. Pulsed and Fourier Transform NMR. Academic Press, Inc., New York.
20. MEIBOOM, S. 1961. *J. Chem. Phys.* **34**:375.
21. EISENBERG, D., and W. KAUZMANN. 1969. Structure and Properties of Water. Oxford University Press, New York. 207, 208, 216.
22. MARQUARDT, D. W. 1959. *Chem. Eng. Prog.* **55**:65.
23. HARTLEY, H. O. 1961. *Technometrics*. **3**:269.
24. MARQUARDT, D. W. 1963. *J. Soc. Indust. Appl. Math.* **11**:431.
25. EISENBERG, D., and W. KAUZMANN. 1969. Structure and Properties of Water. Oxford University Press, New York. 228.
26. RESING, H. A. 1972. *Adv. Mol. Relaxation Processes*. **3**:199.
27. RABIDEAU, S. W., E. D. FINCH, and A. B. DENISON. 1968. *J. Chem. Phys.* **49**:4660.
28. WALTER, J. A., and A. B. HOPE. 1971. *Aust. J. Biol. Sci.* **24**:497.
29. EISENBERG, D., and W. KAUZMANN. 1969. Structure and Properties of Water. Oxford University Press, New York. 209.
30. HARVEY, S. C., and P. HOEKSTRA. 1972. *J. Phys. Chem.* **76**:2987.

31. DERBYSHIRE, W., and J. L. PARSONS. 1972. *J. Mag. Resonance*. **6**:344.
32. FREYMAN, M. and R. FREYMAN. 1951. *C.R. Acad. Sci.* **232**:401, 1096.
33. GOOD, W. 1973. *J. Theor. Biol.* **39**:249.
34. KUNTZ, I. D., and T. S. BRASSFIELD. 1971. *Arch. Biochem. Biophys.* **142**:660.
35. MASSZI, G. 1972. *Acta Biochim. Biophys. Acad. Sci. Hung.* **7**:349.